

Systematic Variation in Structural and Magnetic Properties of BiFeO₃ Nanoparticles by A-site Substitution

*M Tahir¹⁾, Saira Riaz²⁾, M Akram Raza³⁾ and *Shahzad Naseem⁴⁾

^{1), 2), 3), 4)} *Centre of Excellence in Solid State Physics, University of the Punjab, Lahore, Pakistan*

⁴⁾ shahzad.cssp@pu.edu.pk

ABSTRACT

Among various multiferroic materials, bismuth iron oxide (BiFeO₃) is a potential candidate as it has high Neel and Curie temperatures for ferromagnetic and ferroelectric properties. But high leakage current in bismuth iron oxide limits its applications in spintronic and data storage devices. In order to overcome this complexity calcium (Ca) doped BiFeO₃ nanoparticles are prepared using sol-gel method. Concentration of dopant (x in Bi_{1-x}Ca_xFeO₃) is varied as 0.1-0.3. Calcium has ionic radius of 114pm so it replaces bismuth that has ionic radius of 117pm. XRD results show that peak position shifts to higher angles indicating that dopant has been successfully incorporated in the host lattice. At high dopant concentration peaks belonging to bismuth deficient phases are observed. The crystallite size decreases as the dopant concentration is increased to 0.2. Further increase in dopant concentration decreases the crystallite size. Ca doped bismuth iron oxide nanoparticles show ferromagnetic behavior. This ferromagnetic behavior arises due to suppression of spiral spin structure. Increase in dielectric constant and decrease in tangent loss is observed with increase in dopant concentration to 0.2.

1. INTRODUCTION

Bismuth iron oxide (BiFeO₃) crystallizes in ABO₃ type distorted perovskite structure that simultaneously exhibits ferromagnetic and ferroelectric properties. Such perovskite structures have attracted world attraction in various technological applications ranging from photovoltaic devices to spintronic devices. BiFeO₃ exhibits high ferroelectric Curie temperature $T_c=1100K$ and Neel temperature $T_N=640K$ (Fu et al. 2016, Riaz et al. 2014a,b). It has a long range cycloidal spin arrangement of 62nm that results in zero magnetic moment and antiferromagnetic nature. In addition, structural instability and leakage current are also associated with BiFeO₃ (Majid et al. 2015, Shah et al. 2014a,b).

Fortunately, all of these drawbacks associated with BiFeO₃ can be overcome with the help of different elements that can be substituted for Bi site or Fe site or both. Ferroelectric nature in BiFeO₃ comes from 6s² lone pair of electron on Bi site while

ferromagnetic properties come from the presence of uncompensated spins at Fe site. The substitution of different dopants in BiFeO_3 will not only help in overcoming the drawbacks associated with BiFeO_3 but also will help in changing its functional responses in different devices (Gao et al. 2016, Riaz et al. 2014a, Hasan et al. 2016).

Among various dopants, divalent metal cations that replace Bi sites are of particular importance. In this case charge compensation due to difference in valence between the host and dopant gives rise to: 1) Some transformation of Fe^{3+} cations to Fe^{4+} cation; 2) formation of oxygen vacancies 3) coexistence of different crystallographic phases. All of these three competing phenomena give rise to interesting properties that can open its path way for new era devices. Among various divalent dopants, Ca^{2+} cation is of particular importance as its ionic radius (114pm) is close to that of bismuth (117pm) (Riaz et al. 2014a).

Ca doped BiFeO_3 nanoparticles have been synthesized using sol-gel method. Variation in structural, ferromagnetic and dielectric properties are correlated with changes in Ca concentration.

2. EXPERIMENTAL DETAILS

Ca doped BiFeO_3 nanoparticles were synthesized via low cost sol-gel method. Iron nitrate, bismuth nitrate and calcium chloride were taken as precursors. Iron nitrate and bismuth nitrate were dissolved in solvent (ethylene glycol) and heated to obtain Ca doped bismuth iron oxide ($\text{Bi}_{1-x}\text{Ca}_x\text{FeO}_3$) nanoparticles. Detailed sol-gel synthesis is reported earlier (Riaz et al. 2014a,b). Dopant concentration (x) is varied as 0.1, 0.2 and 0.3. Nanoparticles were structurally characterized using Bruker D8 Advance X-ray diffractometer. For magnetic analysis Lakeshore's 7407 Vibrating Sample Magnetometer was used.

3. RESULTS AND DISCUSSION

XRD patterns for Ca doped BiFeO_3 nanoparticles can be seen in Fig. 1. Presence of diffraction peaks corresponding to planes (104), (110), (113), (122), (018), (214), (300), (125) indicate the formation of perovskite structure of BiFeO_3 with rhombohedral distorted unit cell. No diffraction peaks matching with bismuth rich or deficient phases were detected at dopant concentration of 0.1 and 0.2. However, at high dopant concentration of 0.3 peaks corresponding to bismuth deficient phase ($\text{Bi}_2\text{Fe}_4\text{O}_9$) were observed. It can be seen that peak positions corresponding to BiFeO_3 shifts to high diffraction angles thus indicating the decrease in lattice parameters. This decrease in lattice parameters is attributed to smaller ionic radius of Ca^{2+} ions (114pm) as compared to that of Bi^{3+} cations. In addition, strain relaxation takes place as host Bi^{3+} cations are replaced with Ca^{2+} cations with smaller ionic radius (Vagadia et al. 2013). Such relaxation results in shifting of peak positions to high diffraction angles.

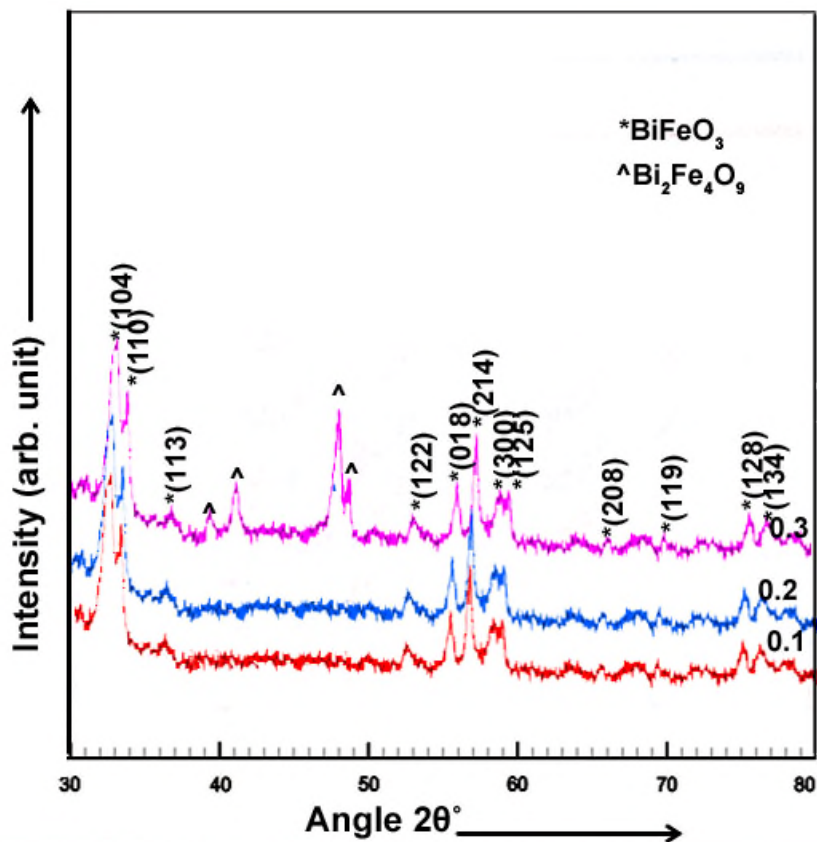


Fig. 1 XRD patterns for Ca doped BiFeO₃ nanoparticles

Tolerance factor was determined using Eq. 1 (Riaz et al. 2015).

$$Tolerance.Factor = \frac{(R_A + R_O)}{\sqrt{2}(R_B + R_O)} \quad (1)$$

Where, R_A is ionic radius of A-site atom, R_B is ionic radius of B site atom, and R_O is ionic radius of oxygen ions. Tolerance factor (Fig. 2) decreases as dopant concentration increases from 0.1 to 0.3. This indicates reduction in Fe-O bond angle with increase in dopant concentration. The total volume is not occupied as Ca²⁺ cations replace Bi³⁺ cations. This results in rotation of oxygen octahedron that increases distortion in the host lattice (Ding et al. 2011).

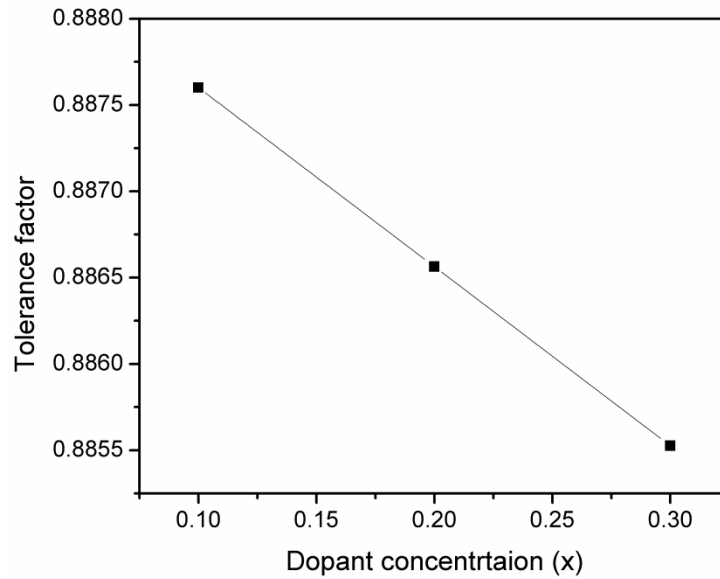


Fig. 2 Tolerance factor for Ca doped BiFeO₃ nanoparticles

Crystallite size (t) (Cullity 1956) and dislocation density (δ) (Kumar et al. 2011) were calculated using Eq. 2-3

$$t = \frac{0.9\lambda}{B \cos \theta} \quad (2)$$

$$\delta = \frac{1}{t^2} \quad (3)$$

Where, θ is the diffraction angle, λ is the wavelength (1.5406Å) and B is Full Width at Half Maximum. Crystallite size and dislocation density are plotted as a function of dopant concentration in Fig. 3. It can be seen that crystallite size increases from 15nm to 18.5nm as dopant concentration increases from 0.1 to 0.2 (Fig. 3(a)). Increase in crystallite size at low dopant concentration (0.1 and 0.2) indicates that Ca atoms are entirely dissolved in the host lattice. However, at high dopant concentration the possibility that Ca atoms occupy the interstitial sites increases. This results in decrease in crystallite size (Riaz et al. 2015). In addition, decrease in crystallite size at dopant concentration 0.3 is attributed to the presence of two different phases of bismuth iron oxide (Fig. 1).

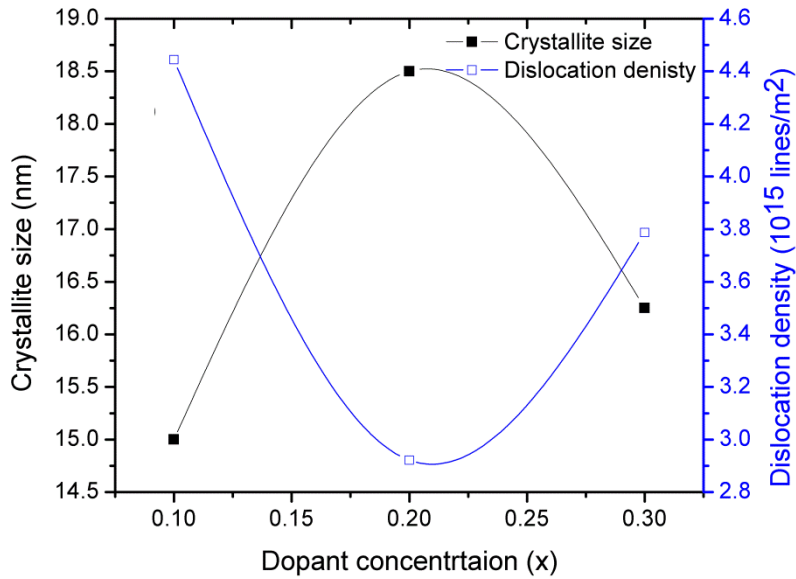


Fig. 3 Crystallite size and dislocation density plotted as a function of dopant concentration

Lattice parameters (a , c) and X-ray density (ρ , g/cm^3) (Cullity 1956) were determined using Eqs. 4-5

$$\sin^2 \theta = \frac{\lambda^2}{3a^2} (h^2 + k^2 + hk) + \frac{\lambda^2 l^2}{4c^2} \quad (4)$$

$$\rho = \frac{1.66042 \Sigma A}{V} \quad (5)$$

Where, ΣA is the sum of atomic weights of the atoms in the unit cell and V is the volume of unit cell in \AA^3 . Lattice parameters and consequently unit cell volume (Table 1) decreases as dopant concentration increases from 0.1 to 0.3. Decrease in unit cell volume is ascribed to slightly lower ionic radius of Ca^{2+} ions in comparison to Bi^{3+} cations. This reduction in unit cell volume then leads to increase in X-ray density of nanoparticles.

Table 1 Structural parameters for Ca doped BiFeO_3 nanoparticles

Dopant concentration (x)	Lattice parameters (\AA)		Unit cell volume (\AA^3)	X-ray density (g/cm^3)
	a	c		
0.1	5.52	14.05	370.7425	8.534037
0.2	5.50	13.99	366.489	8.633083
0.3	5.49	13.93	363.5915	8.701882

Figure 4 shows M-H curves for Ca doped BiFeO_3 nanoparticles. These nanoparticles exhibit ferromagnetic behavior. On the other hand, bulk BiFeO_3 exhibits

antiferromagnetic behavior. Saturation magnetization increases from 0.02223emu to 0.09767emu as dopant concentration increases from 0.1 to 0.2. As dopant concentration was increased to 0.3 saturation magnetization decreased to 0.05254emu. BiFeO₃ has cycloidal spin structure of 62nm and if the crystallite size is less than 62nm BiFeO₃ will not have the random orientations of the spins. This results in ferromagnetic behavior in otherwise antiferromagnetic BiFeO₃. As it was observed in Fig. 3 that crystallite size of Ca doped BiFeO₃ nanoparticles is less than 62nm thus leading to ferromagnetic behavior of Ca doped BiFeO₃ nanoparticles. In addition, replacement of Bi³⁺ with Ca²⁺ cations requires charge compensation mechanism that can take place in two ways: 1) Creation of oxygen vacancies; 2) Conversion of Fe³⁺ cation to Fe⁴⁺ cations. Both of the above-mentioned factors lead to increased magnetization (Riaz et al. 2014b). The decrease in magnetization at high dopant concentration (0.3) is due to Bi₂Fe₄O₉ phase as was observed in Fig. 1. Moreover, tolerance factor (Fig. 2) decreases with increase in dopant concentration thus resulting in distortion in the lattice. This distortion also leads to suppression of spin structure and gives rise to ferromagnetic behavior of BiFeO₃.

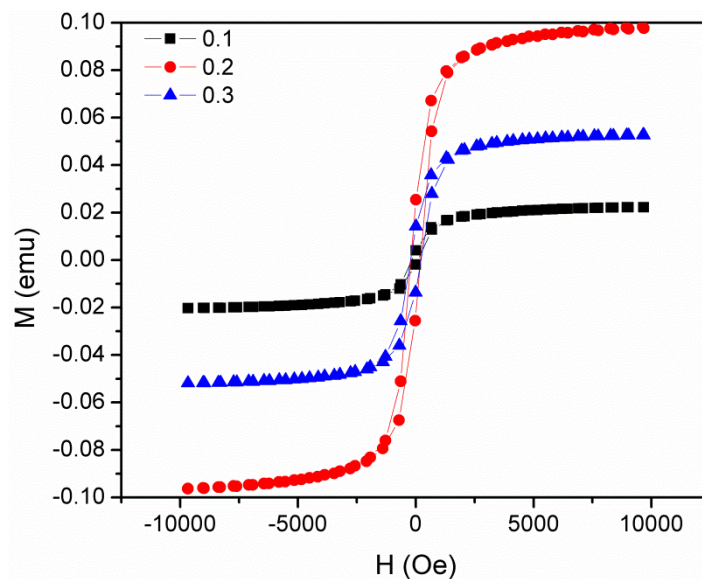


Fig. 4 M-H curves for Ca doped BiFeO₃ nanoparticles

4. CONCLUSIONS

Ca doped BiFeO₃ nanoparticles were prepared using sol-gel method with variation in dopant concentration as 0.1, 0.2 and 0.3. XRD results confirmed the formation of phase pure BiFeO₃ at dopant concentration 0.1 and 0.2 while inclusion of Bi₂Fe₄O₉ was observed as dopant concentration increased to 0.3. Tolerance factor was decreased as dopant concentration was increased indicating the rotation of oxygen octahedron thus increasing distortion in BiFeO₃.

REFERENCES

- Cullity, B.D. (1956), "Elements of x-ray diffraction," Addison Wesley Publishing Company, USA.
- Ding, Y., Wang, T.H., Yang, W.C., Lin, T.C., Tu, C.S., Yao, Y.D., Wu and K.T. (2011), "Magnetization, Magnetoelectric Effect, and Structure Transition in BiFeO₃ and (Bi_{0.95}La_{0.05})FeO₃ Multiferroic Ceramics," *IEEE Trans. Magn.*, **47**, 513.
- Fu, C., Sun, F., Hao, J., Gao, R., Cai, W., Chen, G. and Deng, X. (2016), "The growth, enhanced optical and magnetic response of BiFeO₃ nanorods synthesized by hydrothermal method," *J. Mater. Sci.: Mater. Electron.* DOI 10.1007/s10854-016-4830-9
- Gao, N., Quan, C., Maa, Y., Han, Y., Wu, Z., Mao, W., Zhang, J., Yang, J., Li, X. and Huang, W. (2016), "Experimental and first principles investigation of the multiferroics BiFeO₃ and Bi_{0.9}Ca_{0.1}FeO₃: Structure, electronic, optical and magnetic properties," *Phys. B*, **481**, 45–52
- Hasan, M., Islam, M.F., Mahbub, R., Hossain, M.S. and Hakim, M.A. (2016), "A soft chemical route to the synthesis of BiFeO₃ nanoparticles with enhanced magnetization," *Mater. Res. Bullet.* **73**, 179–186
- Kumar, N., Sharma, V., Parihar, U., Sachdeva, R., Padha, N. and Panchal, C.J. (2011) "Structure, optical and electrical characterization of tin selenide thin films deposited at room temperature using thermal evaporation method," *J. Nano- Electron. Phys.*, **3**, 117-126
- Majid, F., Riaz, S. and Naseem, S. (2015), "Microwave-assisted sol–gel synthesis of BiFeO₃ nanoparticles," *J. Sol-Gel Sci. Technol.* **74**, 329-339.
- Riaz, S., Majid, F., Shah, S.M.H. and Naseem, S. (2014a), "Enhanced magnetic and structural properties of Ca doped BiFeO₃ thin films," *Indian J. Phys.* **88**, 1037–1044.
- Riaz, S., Shah, S.M.H., Akbar, A., Atiq, S. and Naseem, S. (2015), "Effect of Mn doping on structural, dielectric and magnetic properties of BiFeO₃ thin films," *J. Sol-Gel Sci. Technol.* **74**, 310-319.
- Riaz, S., Shah, S.M.H., Akbar, A., Kayani, Z.N. and Naseem, S. (2014b) "Effect of Bi/Fe Ratio on the Structural and Magnetic Properties of BiFeO₃ Thin Films by Sol-Gel," *IEEE Trans. Magn.* **50**, 2201304.
- Shah, S.M.H., Akbar, A., Riaz, S., Atiq, S. and Naseem, S. (2014a), "Magnetic, Structural, and Dielectric Properties of Bi_{1-x}K_xFeO₃ Thin Films Using Sol-Gel," *IEEE Trans. Magn.* **50**, 2201004.
- Shah, S.M.H., Riaz, S., Akbar, A., Atiq, S. and Naseem, S. (2014b), "Effect of Solvents on the Ferromagnetic Behavior of Undoped BiFeO₃ Prepared by Sol-Gel," *IEEE Trans. Magn.* **50**, 2200904.
- Vagadia, M., Ravalia, A., Solanki, P.S., Choudhary, R.J., Phase, D.M. and Kuberkar, D.G. (2013) "Improvement in resistive switching of Ba-doped BiFeO₃ films," *Appl. Phys. Lett.*, **103**, 033504.